

AD-753 693

TIME DOMAIN MEASUREMENT SYSTEM

Harry M. Cronson, et al

Sperry Rand Research Center

Prepared for:

Air Force Avionics Laboratory

December 1972

DISTRIBUTED BY:

**NTIS**

National Technical Information Service  
U. S. DEPARTMENT OF COMMERCE  
5285 Port Royal Road, Springfield Va. 22151

*Handwritten initials*

AD 753693

TIME DOMAIN  
MEASUREMENT SYSTEM

H. M. Cronson, P. G. Mitchell

Sperry Rand Research Center  
Sudbury, Massachusetts

TECHNICAL REPORT AFAL-TR-72-353



*Faint, illegible markings or stamp*

December 1972

Approved for public release; distribution unlimited.

Reproduced by  
NATIONAL TECHNICAL  
INFORMATION SERVICE  
U S Department of Commerce  
Springfield VA 22151

AIR FORCE AVIONICS LABORATORY  
AIR FORCE SYSTEMS COMMAND  
WRIGHT-PATTERSON AIR FORCE BASE, OHIO

## NOTICES

When Government drawings, specifications, or other data are used for any purpose other than in connection with a definitely related Government procurement operation, the United States Government thereby incurs no responsibility nor any obligation whatsoever; and the fact that the government may have formulated, furnished, or in any way supplied the said drawings, specifications, or other data, is not to be regarded by implication or otherwise as in any manner licensing the holder or any other person or corporation, or conveying any rights or permission to manufacture, use, or sell any patented invention that may in any way be related thereto.

ADDITIONAL FOR	
DTIC	White Section <input checked="" type="checkbox"/>
DTG	Blue Section <input type="checkbox"/>
UNANNOUNCED	<input type="checkbox"/>
JUSTIFICATION	.....
BY .....	
DISTRIBUTION AVAILABILITY CODES	
Dist.	AVAIL. and SPECIAL
A	

Copies of this report should not be returned unless return is required by security considerations, contractual obligations, or notice on a specific document.

UNCLASSIFIED

Security Classification

DOCUMENT CONTROL DATA - R&D		
<i>(Security classification of title body of abstract and indexing annotation must be entered when the overall report is classified)</i>		
1 ORIGINATING ACTIVITY (Corporate author) Sperry Rand Research Center 100 North Rd. Sudbury, MA 01776		2a REPORT SECURITY CLASSIFICATION Unclassified
		2b GROUP --
3 REPORT TITLE TIME DOMAIN MEASUREMENT SYSTEM		
4 DESCRIPTIVE NOTES (Type of report and inclusive dates) Final Technical Report - 15 May 1972 to 15 September 1972		
5 AUTHOR(S) (Last name, first name, initial) Cronson, Harry M. Mitchell, Peter G.		
6 REPORT DATE December 1972	7a TOTAL NO OF PAGES 46	7b NO OF REFS 4
8a CONTRACT OR GRANT NO F33615-72-C-2061	9a ORIGINATOR'S REPORT NUMBER(S) SRRC-CR-72-12	
b PROJECT NO 7633	9b OTHER REPORT NO(S) (Any other numbers that may be assigned this report) AFAL-TR-72-353	
c		
d		
10 AVAILABILITY/LIMITATION NOTICES Approved for public release; distribution unlimited.		
11 SUPPLEMENTARY NOTES	12 SPONSORING MILITARY ACTIVITY Air Force Avionics Laboratory Air Force Systems Command Wright-Patterson AFB, Ohio	
13 ABSTRACT <p>This report describes investigations and modifications, both in hardware and software, to improve the accuracy of an AFAL time domain metrology system for measuring the constitutive properties of materials. Experiments revealed that the systematic error observed in the data was due to small mismatches in the connectors adjacent to the material sample. The reflections and the systematic error were reduced by improving the design of one of the connectors and replacing the other delay line and connector by precision air line. Software procedures to further remove the effects of line mismatches from the data were also developed. Two programs, one using a calibrated sample and the other using a displaced short, did not significantly change the already improved results with the modified system. The observed erratic behavior around 100 MHz was investigated and attributed to the large influence of random noise at these frequencies. This low frequency data can be improved by testing thicker samples. Alternative procedures for measuring low loss materials were analyzed and it was concluded that longer material samples were required to increase measurement accuracy.</p>		

Ia

DD FORM 1473  
1 JAN 64

UNCLASSIFIED

Security Classification

14 KEY WORDS	LINK A		LINK B		LINK C	
	ROLE	WT	ROLE	WT	ROLE	WT
Time domain metrology Microwave measurement of materials Coaxial connector mismatch Computer correction of time domain measurements Permeability Permittivity Pulse measurements						

**INSTRUCTIONS**

1. **ORIGINATING ACTIVITY:** Enter the name and address of the contractor, subcontractor, grantee, Department of Defense activity or other organization (*corporate author*) issuing the report.

2a. **REPORT SECURITY CLASSIFICATION:** Enter the overall security classification of the report. Indicate whether "Restricted Data" is included. Marking is to be in accordance with appropriate security regulations.

2b. **GROUP:** Automatic downgrading is specified in DoD Directive 5200.10 and Armed Forces Industrial Manual. Enter the group number. Also, when applicable, show that optional markings have been used for Group 3 and Group 4 as authorized.

3. **REPORT TITLE:** Enter the complete report title in all capital letters. Titles in all cases should be unclassified. If a meaningful title cannot be selected without classification, show title classification in all capitals in parenthesis immediately following the title.

4. **DESCRIPTIVE NOTES:** If appropriate, enter the type of report, e.g., interim, progress, summary, annual, or final. Give the inclusive dates when a specific reporting period is covered.

5. **AUTHOR(S):** Enter the name(s) of author(s) as shown on or in the report. Enter last name, first name, middle initial. If military, show rank and branch of service. The name of the principal author is an absolute minimum requirement.

6. **REPORT DATE:** Enter the date of the report as day, month, year; or month, year. If more than one date appears on the report, use date of publication.

7a. **TOTAL NUMBER OF PAGES:** The total page count should follow normal pagination procedures, i.e., enter the number of pages containing information.

7b. **NUMBER OF REFERENCES:** Enter the total number of references cited in the report.

8a. **CONTRACT OR GRANT NUMBER:** If appropriate, enter the applicable number of the contract or grant under which the report was written.

8b, 8c, & 8d. **PROJECT NUMBER:** Enter the appropriate military department identification, such as project number, subproject number, system numbers, task number, etc.

9a. **ORIGINATOR'S REPORT NUMBER(S):** Enter the official report number by which the document will be identified and controlled by the originating activity. This number must be unique to this report.

9b. **OTHER REPORT NUMBER(S):** If the report has been assigned any other report numbers (*either by the originator or by the sponsor*), also enter this number(s).

10. **AVAILABILITY, LIMITATION NOTICES:** Enter any limitations on further dissemination of the report, other than those

imposed by security classification, using standard statements such as:

- (1) "Qualified requesters may obtain copies of this report from DDC."
- (2) "Foreign announcement and dissemination of this report by DDC is not authorized."
- (3) "U. S. Government agencies may obtain copies of this report directly from DDC. Other qualified DDC users shall request through \_\_\_\_\_."
- (4) "U. S. military agencies may obtain copies of this report directly from DDC. Other qualified users shall request through \_\_\_\_\_."
- (5) "All distribution of this report is controlled. Qualified DDC users shall request through \_\_\_\_\_."

If the report has been furnished to the Office of Technical Services, Department of Commerce, for sale to the public, indicate this fact and enter the price, if known.

11. **SUPPLEMENTARY NOTES:** Use for additional explanatory notes.

12. **SPONSORING MILITARY ACTIVITY:** Enter the name of the departmental project office or laboratory sponsoring (*paying for*) the research and development. Include address.

13. **ABSTRACT:** Enter an abstract giving a brief and factual summary of the document indicative of the report, even though it may also appear elsewhere in the body of the technical report. If additional space is required, a continuation sheet shall be attached.

It is highly desirable that the abstract of classified reports be unclassified. Each paragraph of the abstract shall end with an indication of the military security classification of the information in the paragraph, represented as (TS), (S), (C), or (U).

There is no limitation on the length of the abstract. However, the suggested length is from 150 to 225 words.

14. **KEY WORDS:** Key words are technically meaningful terms or short phrases that characterize a report and may be used as index entries for cataloging the report. Key words must be selected so that no security classification is required. Identifiers, such as equipment model designation, trade name, military project code name, geographic location, may be used as key words but will be followed by an indication of technical context. The assignment of links, rules, and weights is optional.

*Ih*

**TIME DOMAIN  
MEASUREMENT SYSTEM**

**H. M. Cronson, P. G. Mitchell**

Approved for public release; distribution unlimited.

## FOREWORD

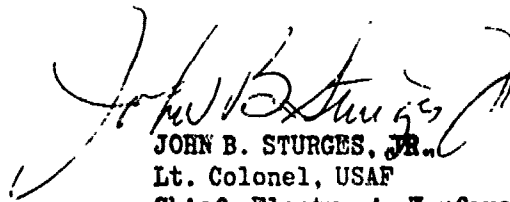
This Final Technical Report covers the work performed under Contract No. F33615-72-C-2061, Project No. 7633, from 15 June to 15 September 1972.

The contract with the Sperry Rand Research Center, 100 North Road, Sudbury, Massachusetts, 01776, is to investigate several techniques for improving the accuracy of an Air Force Avionics Laboratory time domain measurement system for measuring the constitutive properties of radar absorbing materials.

Dr. H. M. Cronson, principal investigator, Mr. P. G. Mitchell, and Mr. R. L. Earle are the SRRC personnel responsible for this contract.

This report was submitted by the authors; October 1972.

This technical Report has been reviewed and is approved for publication.



JOHN B. STURGES, JR.  
Lt. Colonel, USAF  
Chief, Electronic Warfare Division

## TABLE OF CONTENTS

<u>Section</u>		<u>Page</u>
1	INTRODUCTION	1
	1.1 Background	1
	1.2 Tasks	1
2	COAXIAL LINE INVESTIGATION	3
	2.1 Introduction	3
	2.2 Measure of Ripple Magnitude	3
	2.3 Ripple Source	4
	2.4 Methods of Ripple Reduction	6
	2.5 Selection, Fabrication and Testing the Modifications	10
3	LOW FREQUENCY RESPONSE	16
	3.1 Introduction	16
	3.2 Experiments and Results	16
	3.3 The Thick Sample Problem	17
4	CALIBRATION WITH STANDARD SAMPLES	20
	4.1 Introduction	20
	4.2 Analysis	20
	4.3 Measurements Using a Standard Sample	24
	4.4 The Displaced Short Method	24
	4.5 Conclusions and Options	27
5	LOW LOSS DIELECTRIC MEASUREMENTS	29
	5.1 Introduction	29
	5.2 The Long Sample Method	29
	REFERENCES	33
	APPENDIX A	A-1
	APPENDIX B	B-1



## LIST OF ILLUSTRATIONS

<u>Figure</u>		<u>Page</u>
1	Compensation of connector shunt capacitance at the foam/air dielectric interface.	8
2	Connector reflections: a) Original end line reflections b) Reflections from modified connector	9
3	GR 900 air line configuration.	11
4	Comparison of $\epsilon$ and $\mu$ results for original and modified system for Teflon.	13
5	Comparison of $\epsilon'$ results for original and modified system for nylon and ferrite JF-1.	14
6	Pulse generator power supplies.	15
7	Angle ambiguity of $\epsilon'$ for a 0.499 inch Teflon sample computed with: a) Original program b) Modified program	19
8	Reflection and transmission in the presence of a discontinuity.	21
9	Comparison of data with and without displaced short corrections.	26
10	Graph for determination of minimum sample length.	31

## SECTION 1 INTRODUCTION

### 1.1 BACKGROUND

The investigations described in this report were performed at the Sperry Rand Research Center (SRRC) in Sudbury, Mass. for the Air Force Avionics Laboratory (AFAL), Wright-Patterson Air Force Base, Ohio under Contract F33615-72-C-2061 over a period from June through September 1972.

In September 1971 SRRC delivered to AFAL a unique prototype system for measuring the constitutive parameters of materials over the frequency range 0.1 to 10 GHz without disturbing the sample. This system was based on time domain metrology principles where the transient responses of a material to a smoothed impulse serves to characterize the test material. The basic components are a subnanosecond baseband pulse generator, coaxial delay line networks, a sampling oscilloscope, a controller, magnetic tape recorder, and analog-digital interfacing. The time domain responses are measured and recorded on magnetic tape, and a subsequent Fourier transform program yields the desired complex permittivity,  $\epsilon$  and complex permeability,  $\mu$ . More detailed information on this system and its operation is contained in two recent AFAL Technical Reports.<sup>1,2</sup>

During the first year of operation at AFAL, the system has proved to be extremely useful for measuring the constitutive parameters of lossy materials. As a result of usage, certain accuracy limitations were noted in the prototype unit. The objective of this program was to investigate several techniques for improving the accuracy and extending the capability of the AFAL system.

### 1.2 TASKS

The tasks in this investigation fell into four categories:

- a) The primary effort was a coaxial line investigation to reduce the observed systematic error in the calculated values of  $\epsilon$  and  $\mu$ . This included the design and fabrication of necessary modifications.

- b) A study to establish the cause of and to eliminate sporadic low frequency errors.
- c) An investigation of the feasibility of using standard samples, with known  $\epsilon$  and  $\mu$ , to calibrate the system and to develop software to implement this technique.
- d) A study to extend the capability of the system to the measurement of low loss dielectric materials.

Each of these tasks is described in subsequent sections. In addition, a preliminary safety analysis was performed to minimize catastrophic failure.

Dr. Harry M. Cronson was the principal investigator in this program. Mr. Peter G. Mitchell was responsible for hardware modifications and performing experimental measurements. Technical assistance was provided by Mr. Richard L. Earle.

## SECTION 2 COAXIAL LINE INVESTIGATION

### 2.1 INTRODUCTION

The major effort in this contract was the reduction of systematic errors. These errors have the appearance of ripples on a plot of the real and imaginary parts of the relative permittivity,  $\epsilon = \epsilon' - j\epsilon''$ , and the relative permeability,  $\mu = \mu' - j\mu''$ , vs frequency. Unlike ripples caused by random noise, the peaks and valleys of systematic ripples usually occur in the same frequency range regardless of the material tested. The systematic ripples are usually larger than random ripples and cannot be reduced by averaging. The probable cause of these systematic ripples is mismatch in the connector and/or RG331 foam cable in the vicinity of the sampler holder. (The AFAL 10 ns measurement system was constructed from semiflexible RG331 cable in order to achieve a relatively compact configuration.) On the other hand, systematic errors were not observed in the prototype SRRC 2.5 ns system constructed from 14 mm precision air line. Since the connectors to the foam cable present a larger discontinuity than General Radio (GR) air line connectors, this discontinuity could cause the observed ripples.

Our method of approach was to divide the coaxial line investigation into 4 sequential subtasks:

- a) Obtaining a quantitative measure of the magnitude of the ripples of existing systems for comparison with later results.
- b) Determining the cause of the ripples.
- c) Investigating methods of ripple reduction.
- d) Fabrication and testing of the recommended modification.

The remainder of this section describes work done under each subtask.

### 2.2 MEASURE OF RIPPLE MAGNITUDE

To reduce the observed spurious responses in  $\mu$  and  $\epsilon$ , it seemed reasonable to first establish the magnitude of these ripples. These numbers could then serve as a basis of comparison for an improved system. As a measure of the ripples, we sought an easily computed quantity related to the difference between the maximum and minimum observed value of  $\epsilon'$ . The quantity arbitrarily selected and called the percentage ripple,  $R$ , is

defined by

$$R = \frac{\text{Max } [\epsilon'] - \text{Min } [\epsilon']}{\text{Average } [\epsilon]} \times 100\% \quad (1)$$

It should be noted that the observed ripples are due to both random and systematic errors. However, since the systematic errors are usually larger, the above equation furnishes a useful guideline for systematic errors. To avoid extreme points at both ends of the spectrum, where random noise errors are large, the 0.1, 0.2, 0.3 and 9.8, 9.9, and 10 GHz values of  $\epsilon'$  were not included. From available data it was convenient to choose a Teflon<sup>\*</sup> sample of 0.25 inch thickness as a comparative sample. The first three entries in Table I list values of R along with the maximum and minimum values of  $\epsilon'$  for the SRRC prototype 2.5 ns air line system, the RG331 10 ns system taken prior to shipment to AFAL, and recent results taken with the AFAL system. As expected, the percentage ripple of the 2.5 ns air line system is much smaller than the AFAL system.

To begin a meaningful coaxial line investigation before the arrival of the AFAL equipment at SRRC in the final month of the contract, a 10 ns RG331 configuration was fabricated at SRRC. The configuration was first tested with a 2.5 ns window to check it out and later with a full 10 ns window. Values of R of the SRRC, RG331 10 ns configuration for both the 2.5 and 10 ns window are given in Table 1.

It is interesting to note that the 2.5 ns RG331 system displays less ripple than the 10 ns RG331 configuration, although the delay lines are identical. This occurs for two reasons. First, since the 10 ns window gives four times as many frequency points, more extreme points are likely to occur. Secondly, the signal-to-noise ratio (SNR) is larger for the 256 point scan in the 2.5 ns window than the 1024 point scan in the 10 ns window. The other entries in the table will be referred to later.

### 2.3 RIPPLE SOURCE

Tests with the SRRC 10 ns foam cable configuration showed the same type of systematic ripples observed in the AFAL system. An examination of the

\*Registered trademark of the I. E. duPont deNemours and Company.

TABLE 1  
 COMPARISON OF MEASUREMENT SYSTEM RIPPLE  
 ON A 0.25 INCH TEFLON SAMPLE

<u>System</u>	<u>Time Window</u>	<u>ε'</u>	<u>Max f [GHz]</u>	<u>ε'</u>	<u>Min f [GHz]</u>	<u>R</u>	<u>Date &amp; Place of Measurement</u>	
2.5 ns air line	2.5 ns	2.07	2.0	1.95	9.6	6 %	12/70	SRRC
10 ns, 331, AFAL	10 ns	2.25	9.2	1.90	8.1	17.5%	8/71	SRRC
10 ns, 331, AFAL	10 ns	2.21	9.6	1.68	6.1	26.5%	6/72	AFAL
10 ns, 331	2.5 ns	2.10	9.6	1.97	2.0	6.5%	7/72	SRRC
10 ns, 331	10 ns	2.16	9.2	1.94	8.3	11 %	7/72	SRRC
10 ns, air line	10 ns	2.07	0.9	1.88	8.6	9.5%	7/72	SRRC
10 ns, modified	10 ns	2.11	2.0	1.95	6.7	8 %	9/72	SRRC

delay lines using TDR methods failed to reveal any discontinuities in the interior of the RG331 cable. However, the connectors on the RG331 cable adjacent to the sample holder did exhibit reflections of the order of 15 mV peak to peak for a 240 mV input step. Further experiments with one of these connectors showed a reflection coefficient that decreased to only -21 dB in the vicinity of 4 GHz. This mismatch appears large enough to be a major contributor to the observed errors.

As another check to determine whether the connectors were the main source of error another 10 ns configuration was constructed at SRRRC using the superior GR900 air line series connectors with two 5 ns sections of air line. This system furnished two 10 ns time windows but an extra transmission background waveform with the sample in the holder had to be included in the measurement procedure background subtraction. The calculated percentage ripple, R, of this system as shown in Table I was less than the SRRRC 10 ns foam system and considerably less than the AFAL 10 ns system. These results furnished additional evidence that the connector mismatch was the main source of systematic error.

#### 2.4 METHODS OF RIPPLE REDUCTION

From the evidence of the previous section, it was clear that any modification which resulted in a lower mismatch in the connectors adjacent to the sample holder would yield reduced systematic ripples. Three modifications were considered:

- a) Replacing the existing 10 ns and 5 ns RG331 lines by General Radio 14 mm air lines with GR900 connectors.
- b) Improving the design of the RG331 to GR900 connector to reduce the mismatch.
- c) Employing a software correction in the Fortran program for the observed connector mismatch.

The first is an obvious solution since we have already demonstrated that an air line system produces less ripple. However, if this approach were adopted, the 10 foot coiled RG331 cable inside the pulse generator box would have to be replaced by a 10 foot run of air line. The resultant configuration

would extend for 15 feet and involve an undesirable major hardware change. To replace the cables on both sides of the sample holder by air line also seems like an extreme solution, since it is the connectors rather than the cables themselves that cause the mismatch. Therefore, the other two possibilities were carefully examined to determine whether they could be used in place of the complete air line replacement.

The simplest solution appeared to be to improve the existing connector. During the contract to build the prototype material measurement system, the RG331 to GR900 connector was specially designed by SRRC since none with very low SWR were commercially available. The original and modified transition between the 0.5" foam cable and 0.56" air line is shown in Fig. 1. The modifications at the foam-air interface are shown as shaded areas. Although the region throughout the transition was designed to be 50  $\Omega$ , the abrupt transition at the foam-air interface contributes an equivalent shunt capacity which produces the mismatch. It seems however, that some abrupt transition must always be present between the two geometries. Therefore, although one must accept some shunt capacity, the match can be improved by increasing the series inductance at the discontinuity to compensate for the existing capacity. In other words, since the shunt capacity reduces the characteristic impedance  $Z_0$  of the line at the discontinuity, the geometry should be changed to increase  $Z_0$  at the same point. In modifying the connector,  $Z_0$  was increased by reducing the step at the interface and removing some of the foam dielectric at the junction. The compensation was done in steps until the amplitude of the mismatch as observed by TDR techniques reached a minimum. Figures 2(a) and (b) show the return from the AFAL end line connector and the modified connector on the 10 ns cable adjacent to the sample holder, respectively. In both cases the input was a 250 mV step. Returns examined from other unmodified transitions usually showed a response of the order of 15 mV. The photos in Fig. 2 demonstrate the improved match in the modified connector. There remains, however, a residual reflection which can contribute some systematic error.

The third approach to ripple reduction involves measuring the mismatch present and using a computer correction to remove the effects of the



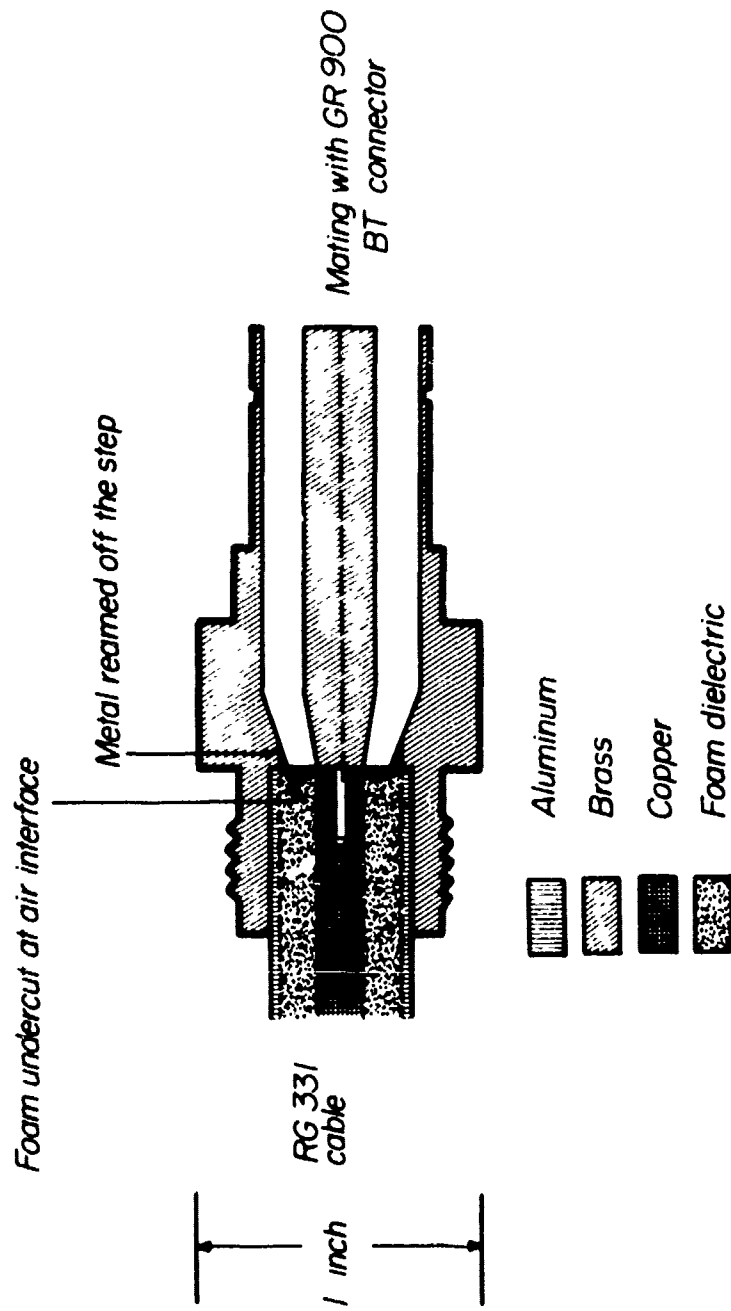
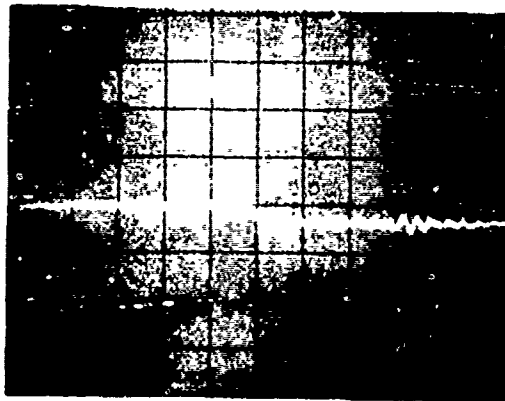
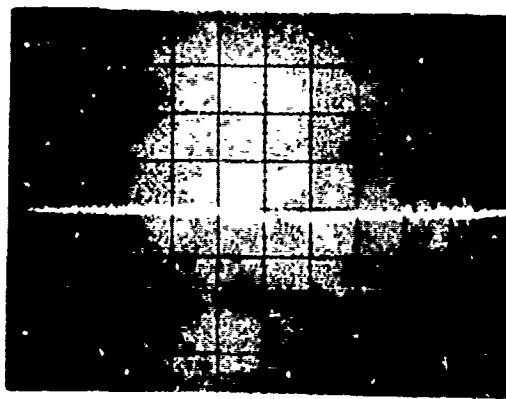


FIG. 1 Compensation of connector shunt capacitance at the foam/air dielectric interface.



(a)



(b)

hor. 250 ps/cm  
 vert. 10 mV/cm

FIG. 2 Connector reflection

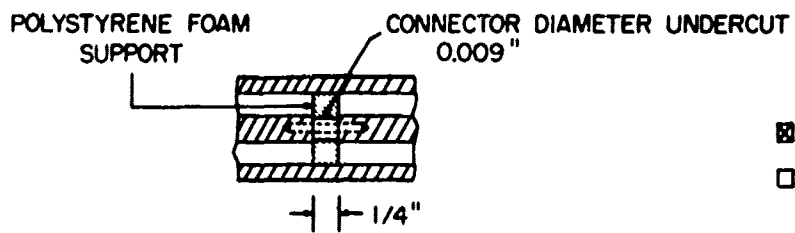
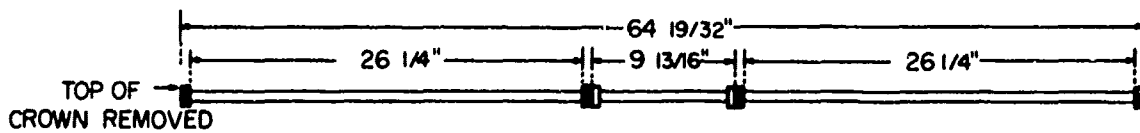
Vert. 10 mV/cm  
 Hor. 250 ps/cm

- a) Original input signal
- b) Reflections from connector

reflection from the final result. Therefore, one could presumably have a poor match in the system, as long as it was known, and calculate a correction for it. A discussion of this problem is presented in Section 4, since the analysis is intimately tied in with calibration with standard samples. The advantage of this method is that even if the line mismatch changes over a period of weeks or months, the procedure will measure the change and correct for it. Disadvantages include the analysis and programming effort required to achieve an operational program, the additional reference waveform required for the computer correction, and the possibility of inconclusive results for small mismatches because of contamination by random noise.

## 2.5 SELECTION, FABRICATION AND TESTING THE MODIFICATIONS

During the investigation, each of the three above methods were studied and evaluated. We decided that a combination of these methods was most likely to produce satisfactory results. First the connector on the 10 ns cable adjacent to the sample holder was modified to compensate for the shunt capacity. This approach was chosen to retain the original pulse generator configuration with the coiled cables inside the box. Secondly, the 5 ns foam end line was replaced by an air line. Unlike air line replacement on the other side of the sample holder, this did not involve a major hardware change and insured an excellent match on the end line side of the holder. Special care was taken in the air line constructed from GR precision tube and rod. The line shown in Fig. 3 consists of 2 long and 1 short section. The middle  $9 \frac{13}{16}$ " section has GR900 AP connectors on each end. Each  $26\frac{1}{4}$ " section has GR900BT connectors on each end which provide support for the inner conductor. The upper portion of the crown was removed from one of these connectors to mate with the sample holder. The long inner conductors are also supported at the center of each line by a  $\frac{1}{4}$ " polystyrene disk. To compensate for the increase in capacitance at the disk, the diameter of the center conductor was reduced as illustrated in Fig. 3. Experiments showed negligible reflections from the completed line. The air line is supported by an I beam with moveable saddle support pieces. Thirdly, to remove the effects of any residual reflections, a computer program was written and included in a modified Fortran routine for the measurement sequence.



- ▣ TYPE 900BT CONNECTORS
- TYPE 900AP CONNECTORS

CENTER CONDUCTOR JOINT AND SUPPORT IN THE MIDDLE OF THE 26  $\frac{1}{4}$ " SECTIONS.

FIG. 3 GR 900 air line configuration.

The above modifications were made on part of the AFAL system returned to SRRC in mid-August and resulted in a reduction of systematic error. Since the connector modification reduced the mismatch to a very low level, no significant improvement was noted when the computer correction was applied and, therefore, the data in the remainder of this section is shown without software correction. Figure 4 shows a comparison of the complex  $\mu$  and  $\epsilon$  for the original system (Fig. 55, Ref. 1) and the improved system. Note the absence of the large variations around 3 GHz originally present. The poorer low frequency values for the improved system are random variations due to noise. The percentage ripple R computed for the modified system (which on different days varied between 7.5% and 9% - the most common value of 8%) is included in Table 1. Another before and after comparison is illustrated in Fig. 5 where the real part of  $\epsilon$  for nylon and a ferrite is plotted for the AFAL system after it was returned to SRRC and the improved system. The AFAL equipment returned to SRRC had an obvious discontinuity in the outer conductor of a connector near the sample holder. The data in Fig. 4 was taken after the connector was realigned and mating surfaces cleaned. These comparisons between the improved and original system illustrate the reduction in systematic error achieved in the coaxial line investigation.

Several improvements, not required by the contract, were made on the components in the pulse generator box of the AFAL system. The avalanche transistor module was rebuilt to have superior physical design. The lantern battery bias supply for the step recovery diodes was replaced by a dc power supply, and a fuse was installed in the power line. Figure 6 now shows the new power supply block diagram. The RG331 foam line between the sample head and sample holder was replaced by another RG331 line whose impedance was closer to 50 ohms.

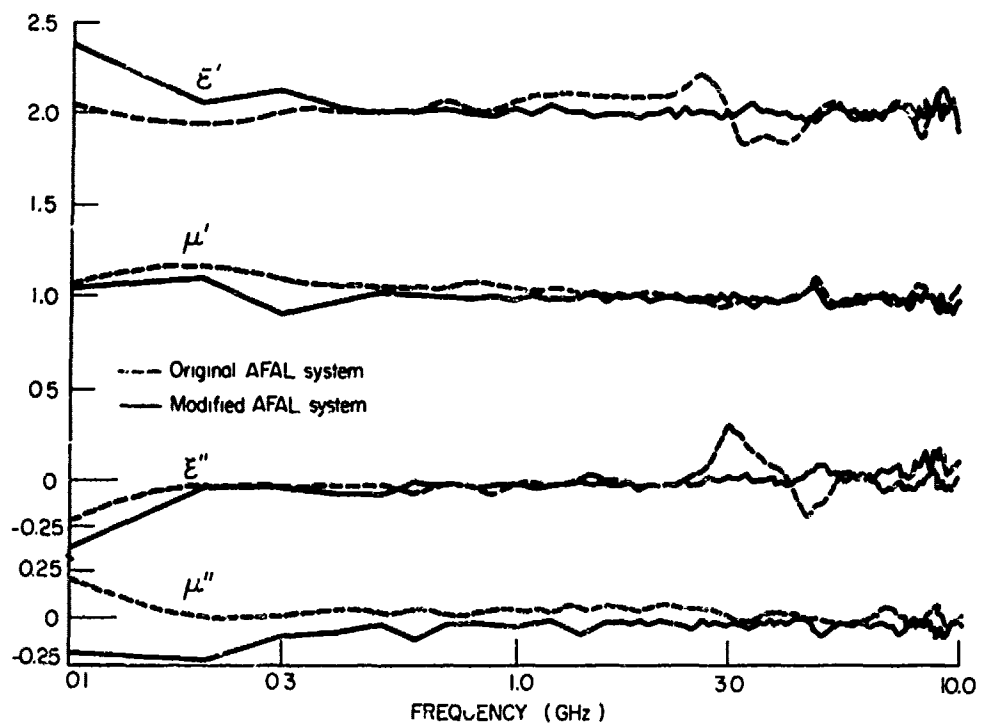


FIG. 4 Comparison of  $\epsilon$  and  $\mu$  results for original and modified system for Teflon.

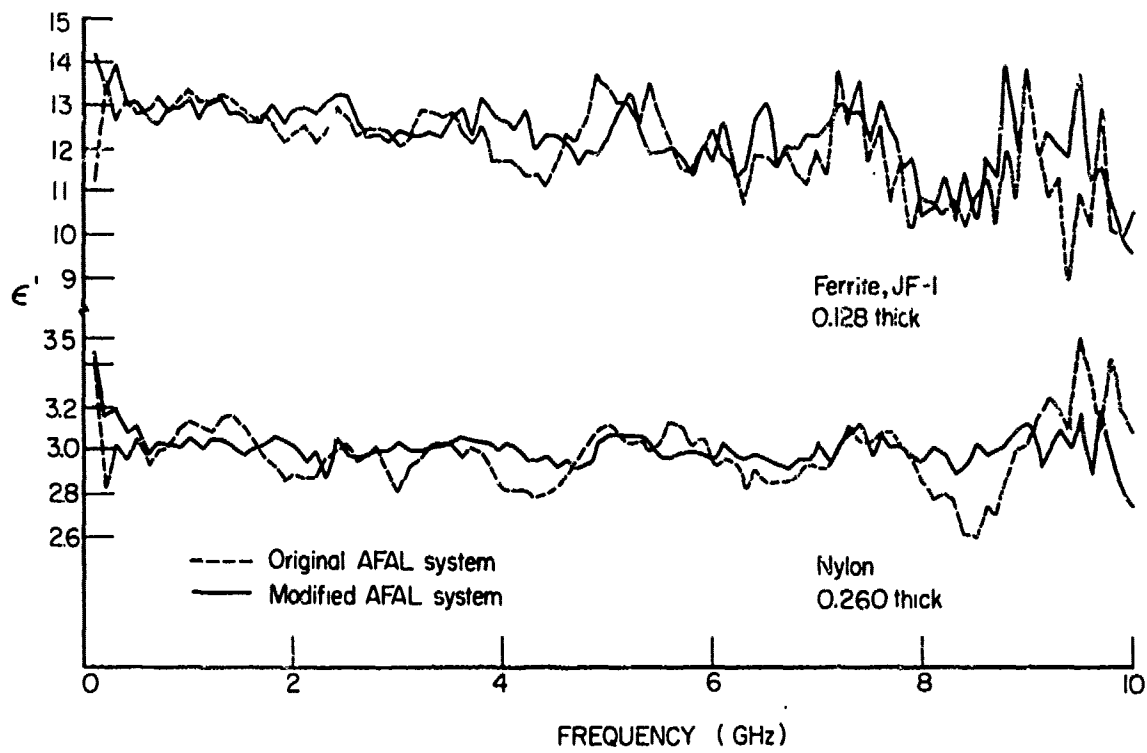


FIG. 5 Comparison of  $\epsilon'$  results for original and modified system for nylon and ferrite JF-1.

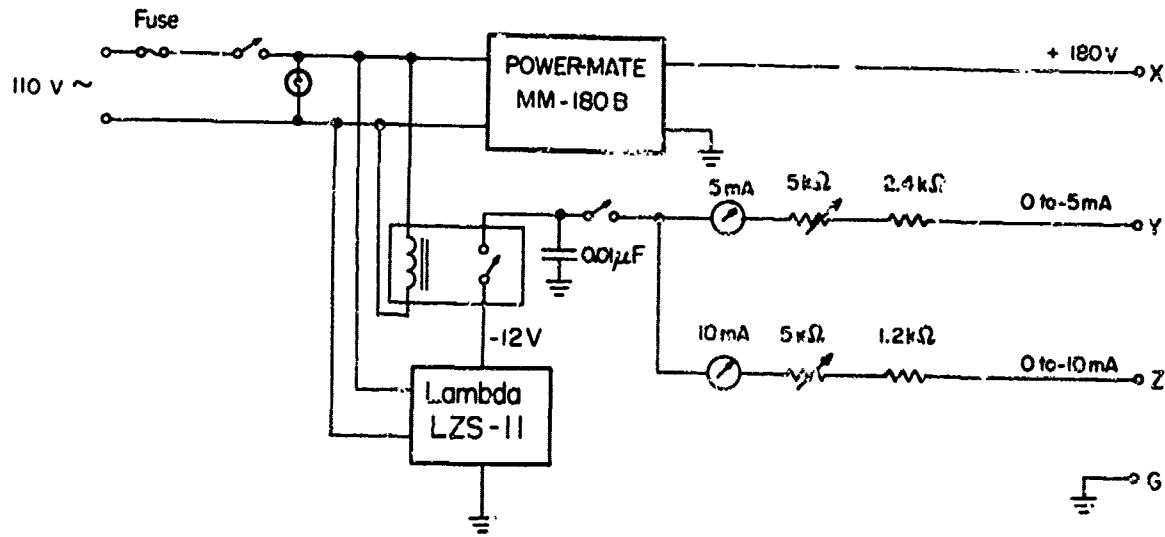


FIG. 6 Pulse generator power supplies.



SECTION 3  
LOW FREQUENCY RESPONSE

3.1 INTRODUCTION

Data below about 500 MHz usually appears more erratic than results at high frequencies. Some reasons for these randomly occurring values could be in setting the reference points, positioning the sample, or noise. Since it has been noted that repetitive runs on the same undisturbed sample also display erratic low frequency data points, the most probable cause is random noise.

The effects of random noise in  $S_{11}$  and  $S_{21}$  are more serious at the lowest frequencies where  $S_{11}$  is near 0 and  $S_{21}$  is near 1. The reason for this is that since the calculations of  $\mu$  and  $\epsilon$  depend essentially on  $S_{11}$  and  $1-S_{21}$ , the same additive errors in these quantities produce much larger percentage errors when  $S_{11}$  is near 0 and  $S_{21}$  is near 1. This can be illustrated by a simple example using experimental values of  $|S_{11}|$  and  $|S_{21}|$ .

TABLE 2  
SCATTERING PARAMETER ERRORS

FREQ.	$ S_{11} $	$ S_{21} $	ASSUMED ADDITIVE ERROR	% ERROR $ S_{11} $	% ERROR $1- S_{21} $
100 MHz	0.009	0.995	0.001	11%	20%
3000 MHz	0.196	0.974	0.001	0.5%	4%

Thus one would certainly expect more error at 100 than 3000 MHz. Of course a more complete error analysis would have to account for phase errors also, but the above illustrates the main point.

3.2 EXPERIMENTS AND RESULTS

The previous example suggests that the low frequency behavior can

be improved if the SNR is increased. However, the price paid for better SNR at lower frequencies is usually poorer SNR at higher frequencies. One method to increase the low frequency SNR is to use a material with a large dielectric constant as a test sample to check the system. One notes, for example, that ferrite samples usually exhibit a fairly flat low frequency response. This method is, of course, inapplicable if the low frequency behavior of a particular material, such as Teflon is desired. A wider excitation pulse will also furnish a higher low frequency SNR. An experiment was performed with a 250 ps pulse which had about 12 dB more spectral amplitude than the 60 ps pulse at low frequencies. As expected, the data showed a smoother lower frequency response with much more erratic high frequency values. To use this method would require another pulse generator or waveform integrator in the system. Perhaps the simplest approach to improve low frequency behavior is the use of a thicker sample that will give more reflection and less transmission than a shorter sample. However, in addition to the poorer high frequency SNR a longer sample can produce a singularity in  $\mu$  and  $\epsilon$  when the sample thickness approaches a half wavelength. It has also been observed that after the singularity, the values of  $\mu$  and  $\epsilon$  are grossly incorrect. Since the longer sample approach appeared most advantageous, more analysis was done to see if the response around and after the discontinuity could be improved.

### 3.3 THE THICK SAMPLE PROBLEM

The values of  $\mu$  and  $\epsilon$  are erratic in the neighborhood of the singularity for the same reason that they are erratic at low frequencies. Namely,  $S_{11}$  is near 0 and  $S_{21}$  is close to 1. In fact, the response is usually worse since the SNR of the incident signals is usually lower near the higher frequency singularity than the one at zero frequency. The singularity cannot be avoided with the present program since division by  $S_{11} \cong 0$  occurs. Although data in the region around the singularity will continue to be erratic, one should be able to improve the values of  $\mu$  and  $\epsilon$  above the singular frequency.

An examination of the present program revealed that  $\mu$  and  $\epsilon$  above the singularity were incorrect because the argument of the quantity  $z = \exp$

$(-j\omega\sqrt{\mu'\epsilon'}d/c)$ , where  $d$  is the sample thickness, (see also Eq. (2), p. 3, Ref. 2), hereafter referred to as  $\arg z$ , was not computed correctly for  $\arg z$  less than  $-\pi$ . If  $\arg z$  is wrong,  $c_2$  (Eq. (9), p.5, Ref. 2) and therefore  $\mu'\epsilon'$  will also be incorrect. A study of Eqs. (2) through (6) in Ref. 2 also showed that the singularity occurs when  $\arg z = -\pi$ . The incorrect values occurred because the arctangent routine that computed  $\arg z$  only yielded angles between  $\pm\pi$ . Thus for  $z$  in the third quadrant, the program gave  $\arg z = \alpha$ , whereas the correct  $\arg z$  should have been  $\alpha - 2\pi$ . To correct this, a change was made in the subroutine CPLEX to give  $\arg z$  between 0 and  $-2\pi$ . The modification is listed in Appendix B. This revised program was tried and yielded the correct values of  $\arg z$ . Figure 7(a) and (b) offers the comparison between  $\epsilon'$  for a 0.499 inch Teflon sample computed with the original program and the modified program. Note that the region of grossly incorrect values for  $\epsilon'$  extends for a considerable frequency interval on both sides of the singularity at 8.4 GHz. This is probably due to the decreased SNR of  $1-S_{21}$  for the longer sample at higher frequencies. It should be mentioned that the revised subroutine will still give incorrect angles for  $\arg z < -2\pi$ . A more involved program change is required to track the phase beyond one complete revolution.

If very accurate data is desired at both low and high frequencies, one could test both a thin and thick sample of the same material. The low frequency data would be furnished by the thick sample, while the thinner sample would supply the higher frequency results.

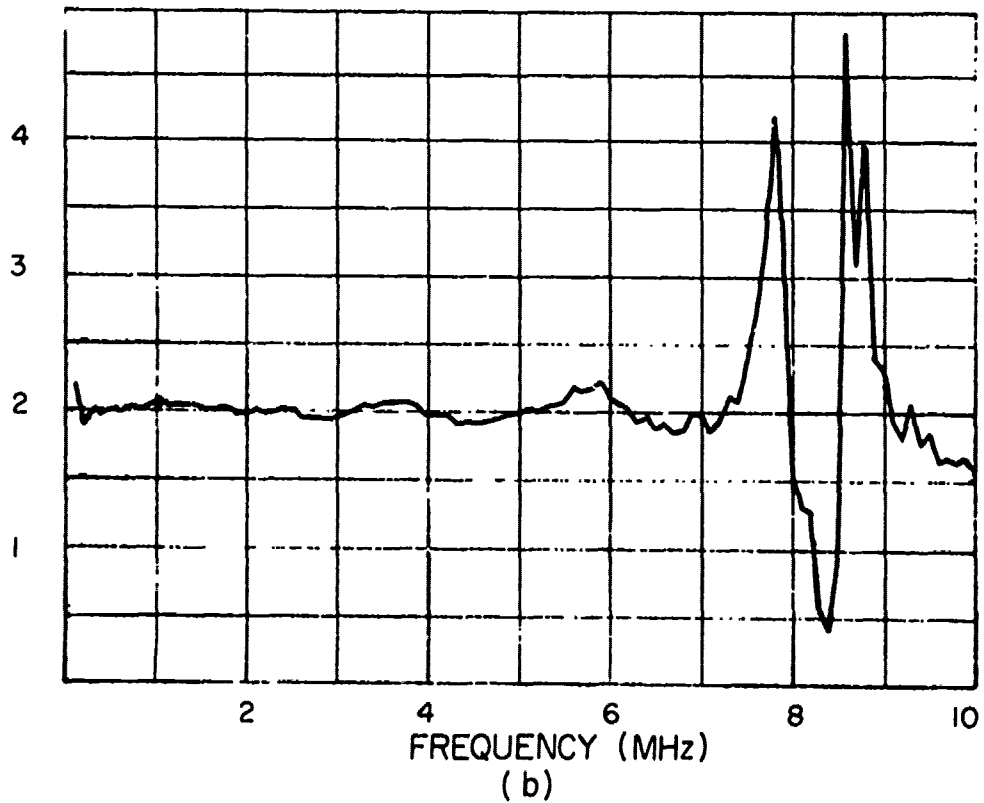
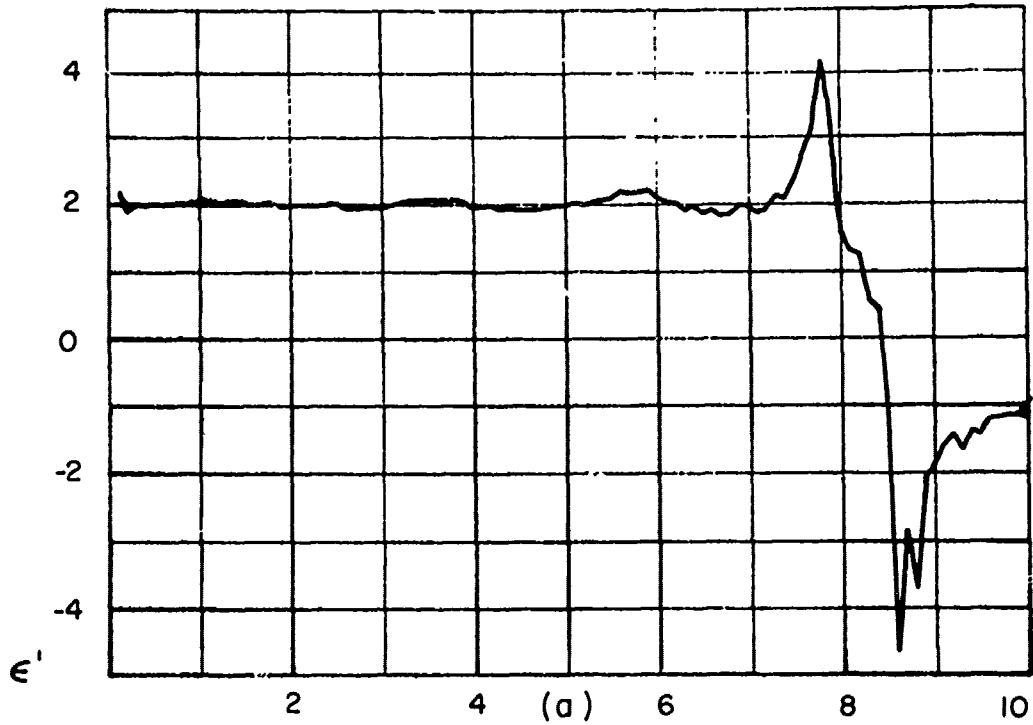


FIG. 7 Angle ambiguity of  $\epsilon'$  for a 0.499 inch Teflon sample  
 computed with  
 a) Original program  
 b) Modified program

SECTION 4  
CALIBRATION WITH STANDARD SAMPLES

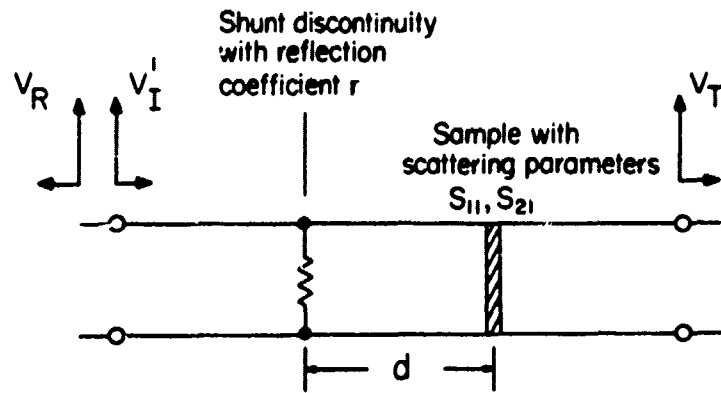
4.1 INTRODUCTION

Another approach investigated to reduce the systematic ripples was based on software correction. For example, it should be possible to employ a standard sample and deduce a system correction factor by comparing the measured to known values. Although computer techniques appeared feasible, our plan of attack was to first reduce mismatches as much as possible via hardware improvements, i.e. connector modification and line replacement, and then to try the software correction on any remaining residual reflections. This plan was adopted because we felt in the short contract period, the hardware modifications showed the greatest probability of success. As it turned out, after the hardware modifications reduced the ripple to a lower value, the subsequent software correction did not significantly improve the results.

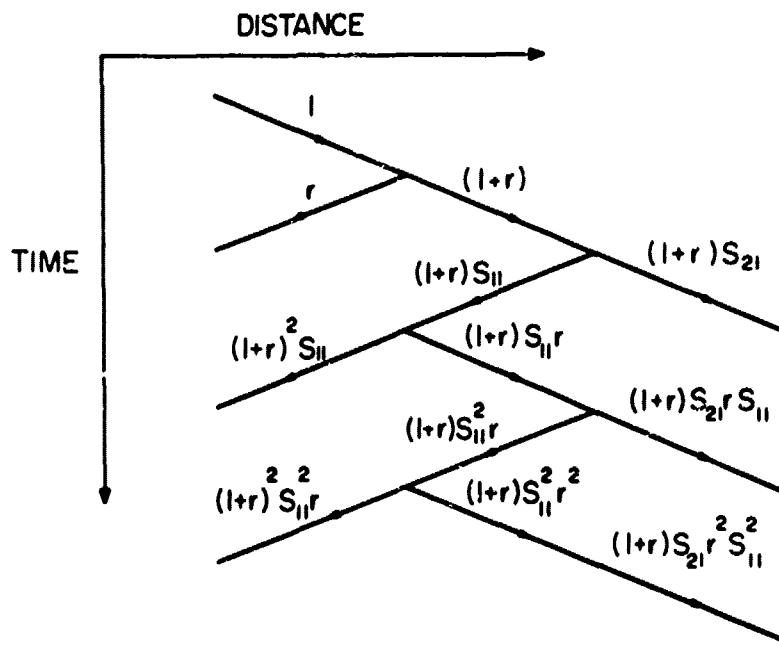
4.2 ANALYSIS

In order to calculate a correction factor, one has to determine the relationship between the measured and true values. One of the simplest models for line mismatch is shown in Fig. 8(a) for a single shunt discontinuity with reflection coefficient  $r(\omega)$  a distance  $d$  to the left of the sample. Fortunately this model should be a good approximation to the modified system where the air line to the right of the sample contributes almost no discontinuity while the modified connector to the left of the sample contributes a small shunt discontinuity. The bounce diagram generated by this configuration is shown in Fig. 8(b), where  $V_R(\omega)$  and  $V_T(\omega)$  are the reflected and transmitted signals respectively at a particular frequency, and,  $S_{11}(\omega)$  and  $S_{21}(\omega)$  are the true values of the scattering parameters. Summing all the reflected signals except the first gives

$$\begin{aligned} V_R &= +(1+r)^2 S_{11} z \left[ 1 + rzS_{11} + (rzS_{11})^2 + \dots \right] \\ &= \frac{S_{11}(1+r)^2 z}{1-rzS_{11}} \end{aligned} \quad (1)$$



(a) Line with shunt discontinuity



(b) Bounce diagram

FIG. 8 Reflection and transmission in the presence of a discontinuity.

where  $z = \exp(-2j\omega d/v)$  and  $v$  is the propagation velocity in the line. The first reflection,  $r$ , is not included since it arises from a part of the time waveform before the reflection time window. Similarly the sum of the transmitted phasors are

$$\begin{aligned} V_T &= S_{21}(1+r) \left[ 1 + rzS_{11} + (rzS_{11})^2 + \dots \right] \\ &= \frac{S_{21}(1+r)}{1-rzS_{11}} \end{aligned} \quad (2)$$

In the experimental procedure, the measured value of the scattering coefficient,  $S_{11}^m$ , is found from ratio

$$S_{11}^m = \frac{V_R - V_{RB}}{V_{RI} - V_{RB}} \quad (3)$$

where the background signal,  $V_{RB}$ , is found from  $V_R$  with  $S_{11} = 0$ , giving

$$V_{RB} = 0 \quad (4)$$

The incident waveform,  $V_{RI}$ , is found by placing a short at the sample position, or equivalently setting  $S_{11} = -1$ . The signal measured is the negative of the incident phasor. Therefore,

$$V_{RI} = \frac{(1+r)z^2}{1+rz} \quad (5)$$

Substituting (1), (4) and (5) into (3) gives

$$S_{11}^m = S_{11} \frac{1+\rho}{1-\rho S_{11}} \quad (6)$$

where we have defined  $\rho = rz$  and call it "the correction factor". Actually  $\rho$  is simply the reflection coefficient looking into the line at the sample position.

Similarly the measured value of the scattering parameter,  $S_{21}^m$ , is

found experimentally from

$$S_{21}^m = \frac{V_T - V_{TB}}{V_{TI} - V_{TB}} \quad (7)$$

The background wave in the transmission window is found by removing the sample and terminating the line, i.e. setting  $S_{21} = 0$ , giving

$$V_{TI} = 0 \quad (8)$$

The incident signal,  $V_{TI}$  is measured with the sample removed or equivalently setting  $S_{21}=1$  and  $S_{11}=0$  yielding

$$V_{TI} = (1+r) \quad (9)$$

Substituting Eqs. (2), (8), and (9) into (7) gives

$$S_{21}^m = \frac{S_{21}}{1-\rho S_{11}} \quad (10)$$

The result is that Eqs. (6) and (10) provide the desired relations between the measured and actual values of the scattering coefficients in terms of the correction factor  $\rho$ . It should be mentioned that although the expressions were derived for a single shunt discontinuity they are also valid for any line reflections describable by a reflection scattering parameter  $A_{11}(\omega)$ , simply by replacing  $\rho$  by  $A_{11}$ . The correction factor  $\rho$  can be found from known and measured values of a standard sample by rewriting Eq. (6) as

$$\rho = \frac{S_{11}^m - S_{11}}{S_{11}(1+S_{11}^m)} \quad (11)$$

After  $\rho$  has been determined from the standard sample for each frequency, it can then be used to correct the measured values  $S_{11}^m$  and  $S_{21}^m$  of any sample.



#### 4.3 MEASUREMENTS USING A STANDARD SAMPLE

A computer program was written so that the correction factor  $\rho$  was computed from a standard sample using Eq. (11) and subsequent corrections applied to other samples. A 0.25 inch thick Teflon sample was used as a standard with an assumed  $\epsilon = 2.03 + j0$  and  $\mu = 1 + j0$ . The actual values of  $S_{11}$  and  $S_{21}$  for Teflon were computed from Eqs. (1) through (4) of Ref. 2. The results were somewhat disappointing since the corrected data did not display significantly less ripple than the uncorrected data. Several reasons can be advanced for this behavior. In the first place, the experiments were performed with configurations exhibiting quite low reflections. Thus there was little error to correct and any corrections that did survive could suffer serious noise contamination. Secondly we had to assume an  $\epsilon$  and  $\mu$  for the standard sample. If the choice was incorrect, it might contribute more error than was originally present. Because of these problems another method was sought which might provide better results.

#### 4.4 THE DISPLACED SHORT METHOD

In the previous analysis a standard sample is used to find a correction factor for the line. However, to characterize the line, a standard sample is not necessary since two measurements on a short and displaced short will accomplish the same task. The displaced short also minimizes several disadvantages of the previous approach. In the first place the SNR of the reflected wave is higher since the signal is larger. Secondly, no assumptions are necessary about the short's parameters except that its reflection coefficient is -1.

The relation between  $\rho$  and displaced short measurements can be found from the previous equations. If the short is a distance  $d_1$  from the discontinuity, the reflected wave is given by an equation similar to (5),

$$V_{R1} = - \frac{(1+r)^2 z_1}{1+r z_1} \quad (12)$$

where  $z_1 = \exp(-2j\omega d_1/v)$ . If the short is now displaced an additional

distance  $D$  to the right, so its new distance,  $d_2$  from the discontinuity is given by

$$d_2 = d_1 + D$$

the reflected wave is now

$$V_{R2} = - \frac{(1+r)^2 z_2}{1+rz_2} \quad (13)$$

The ratio of the two reflections,  $V$ , is

$$V = \frac{V_{R1}}{V_{R2}} = \frac{z_1(1+rz_2)}{z_2(1+rz_1)} = \frac{\frac{z_1}{z_2} + \rho}{1 + \rho} \quad (14)$$

where as before,  $\rho = rz_1$ . Noting  $z_1/z_2 = \exp(2j\omega D/v)$  the correction factor can be found from the measured ratio and the calculated value of  $z_1/z_2$  as

$$\rho = - \frac{V - e^{\frac{2j\omega D}{v}}}{V - 1} \quad (15)$$

Another program was written to compute  $\rho$  from Eq. (15) rather than (11). To obtain the necessary data on the displaced short,  $V_{R2}$ , another reference waveform was acquired. Experiments using the displaced short method, as in the calibrated sample method, did not show significant variations between the corrected and uncorrected values. Figure 9 illustrates values obtained for  $\epsilon'$  with and without the displaced short correction for nylon and ferrite. To study possible differences, comparisons were made on data taken on different days to separate random from deterministic errors. A careful examination revealed that some of the systematic error was reduced by the correction, while other apparently systematic errors remained. We hypothesized that the residual mismatch is so small that software correction does not make much difference.

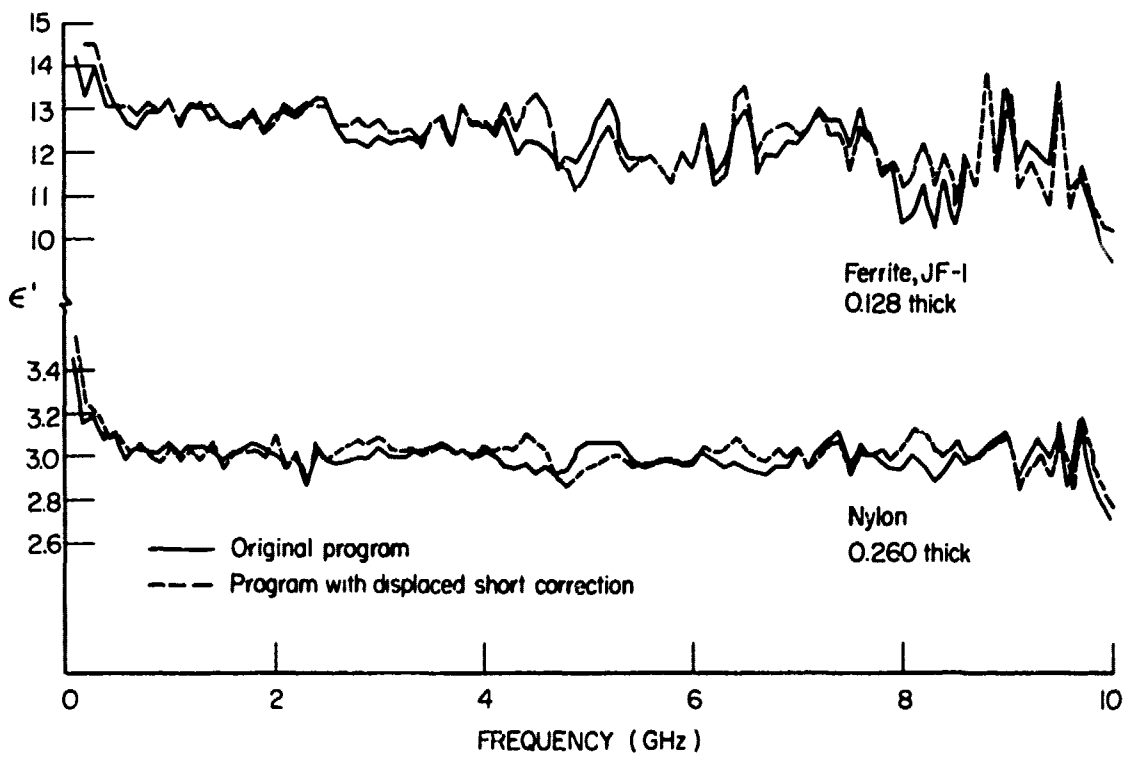


FIG. 9 Comparison of data with and without displaced short corrections.

To determine whether the correction was working at all, we purposely introduced a large mismatch in the line by inserting a Teflon disk against the sample holder connector. The results showed the displaced short procedure was indeed reducing the systematic error. For example, a measurement on nylon with the uncorrected data gave a percentage ripple,  $R = 33\%$ , whereas the corrected data gave  $R = 17\%$ . It should be stressed that efforts to reduce the systematic error do not reduce the random error. Therefore, the erratic results at lower frequencies, which are due to noise, are not improved by either the calibrated sample or displaced short procedure.

#### 4.5 CONCLUSIONS AND OPTIONS

In conclusion, we have demonstrated the feasibility of reducing systematic error by computer correction. However, since the mismatch was already reduced to a low level by hardware corrections, additional improvement by software techniques in the modified system was nearly imperceptible. Of the two correction methods developed, the displaced short seems superior because of the larger SNR of its waveforms and the fact that no constitutive parameters are required.

In Appendix A, we have included a revised main program to compute  $\mu$  and  $\epsilon$  with the displaced short procedure. The operator has the option of scanning the waveforms as described in Ref. 1 and using the original Fortran program or including the displaced short waveform with the revised program. The only change in the measurement procedure is the acquisition of another reference waveform after the incident waveform in the R window is scanned. The revised procedure below should be inserted after the B6 operating sequence as given on p. 18 of Ref. 1 and before step B7.

#### Displaced Short Waveform Modification

B6A COAX(R) is lit

The metal short already in place in the coaxial line 1 inch from the incident connector should now be positioned with the supplied gauge block 1.4 inches from the incident connector.

To continue, push SHORT  
Data from the scan in step B6 will first be written on tape if  
WRITE (red) is lit, and SHORT REFL (red) will again be lit  
during the scan.

B7 COAX(R) is lit  
Continue original operating sequence

We have demonstrated that software corrections are feasible, but do  
not significantly improve results if the residual mismatch is small.

## SECTION 5 LOW LOSS DIELECTRIC MEASUREMENTS

### 5.1 INTRODUCTION

A secondary task during this contract was the investigation of techniques for adapting the AFAL measurement system to low loss dielectric materials. Materials with loss tangent as small as  $10^{-3}$  are of interest, particularly over the frequency range 1 to 10 GHz. The prototype AFAL system was designed to measure  $\epsilon$  and  $\mu$  with errors of the order of  $\pm 0.1$ . Although these errors are acceptable for testing high loss RAM type materials, they are too large for specifying losses in radome type materials. Low loss measurements are inaccurate because the loss introduced by the nominal 0.25 inch samples is smaller than the measurement uncertainty. For example, a signal transmitted through a 0.25 inch sample of a material with  $\epsilon' = 2$  and  $\tan \delta = 10^{-3}$  is attenuated by about 1 part in  $10^4$  at 1 GHz. If the incident signal has an SNR of 60 dB, which translates into a measurement uncertainty of approximately 1 part in  $10^3$ , then the uncertainty is 10 times larger than the quantity we seek to determine. Obviously no meaningful measurement can be made in this situation.

### 5.2 THE LONG SAMPLE METHOD

One obvious way to increase measurement accuracy is to introduce more transmission loss by using a longer sample. A convenient geometry for time domain measurements is a sample of material completely filling the transmission line backed by a short circuit. For this configuration the first reflection from the air-dielectric interface is used to determine  $\epsilon'$ , while the second reflection, which traverses the sample twice, gives  $\epsilon''$ .

The relation between the sample attenuation and measurement uncertainty can be found from the following expressions. The total dielectric loss,  $\alpha$ , for the TEM propagation mode is given in dB by Ref. (3),

$$[\alpha] = 4.62 Fd/\epsilon' \tan \delta \quad (16)$$

where  $F$  is in GHz,  $d$  is the sample length in inches and the notation is

introduced where square brackets around a quantity denote dB, i.e.  $[\alpha] = 20 \log_{10} \alpha$ . The transmission loss of the material is computed from the ratio of the Fourier transform of the transmitted incident waveform. These waveforms are contaminated with noise. If gaussian noise is assumed, the standard deviation,  $\sigma$ , of the error is given in dB by Ref. (4)

$$[\sigma] \cong \frac{8.7}{S_i} (1 + \alpha^2)^{1/2} \quad (17)$$

where  $S_i$  is the SNR of the incident wave. Note that both  $S_i$  and  $\alpha$  are expressed in Eq. (17) as voltage ratios. Equation (17) is a valid approximation for  $S_i/\alpha \gtrsim 10$ . The criterion for accurate measurements is  $[\alpha] \gg [\sigma]$ .

Equations (16) and (17) can be used along with the incident SNR to determine what sample lengths are required for good measurements. For example, suppose one desires to measure a dielectric with  $\epsilon' = 2$  and  $\tan \delta = 10^{-3}$ . What minimum length is required to measure this material over the frequency range 1 to 10 GHz, such that  $[\alpha] \geq 10 [\sigma]$  over the entire range? The problem can be solved graphically using the experimentally determined incident SNR found in Table 3.

TABLE 3  
INCIDENT SNR FOR VARIOUS FREQUENCIES

Freq. (GHz)	1	3	5	8	10
Incident SNR (dB)	62	59	54	48	37

Since  $\alpha$  will be close to 1 for a  $\tan \delta = 10^{-3}$  material, Eq. (17) can be approximated by  $[\sigma] \cong 12.3/S_i$ . This quantity is plotted in Fig. 10 along with  $10 [\sigma]$ . As a first trial, a length  $d = 12''$  is chosen, and  $[\alpha]$  computed from Eq. (16) and plotted. The graph shows that the inequality  $[\alpha] \geq 10 [\sigma]$  is not satisfied at the low and high frequency end. A new  $d$  of  $27''$  is determined by setting  $[\alpha]$  equal to  $10 [\sigma]$  at 10 GHz. As shown in Fig. 10, the  $27''$  length satisfies the inequality over the entire frequency

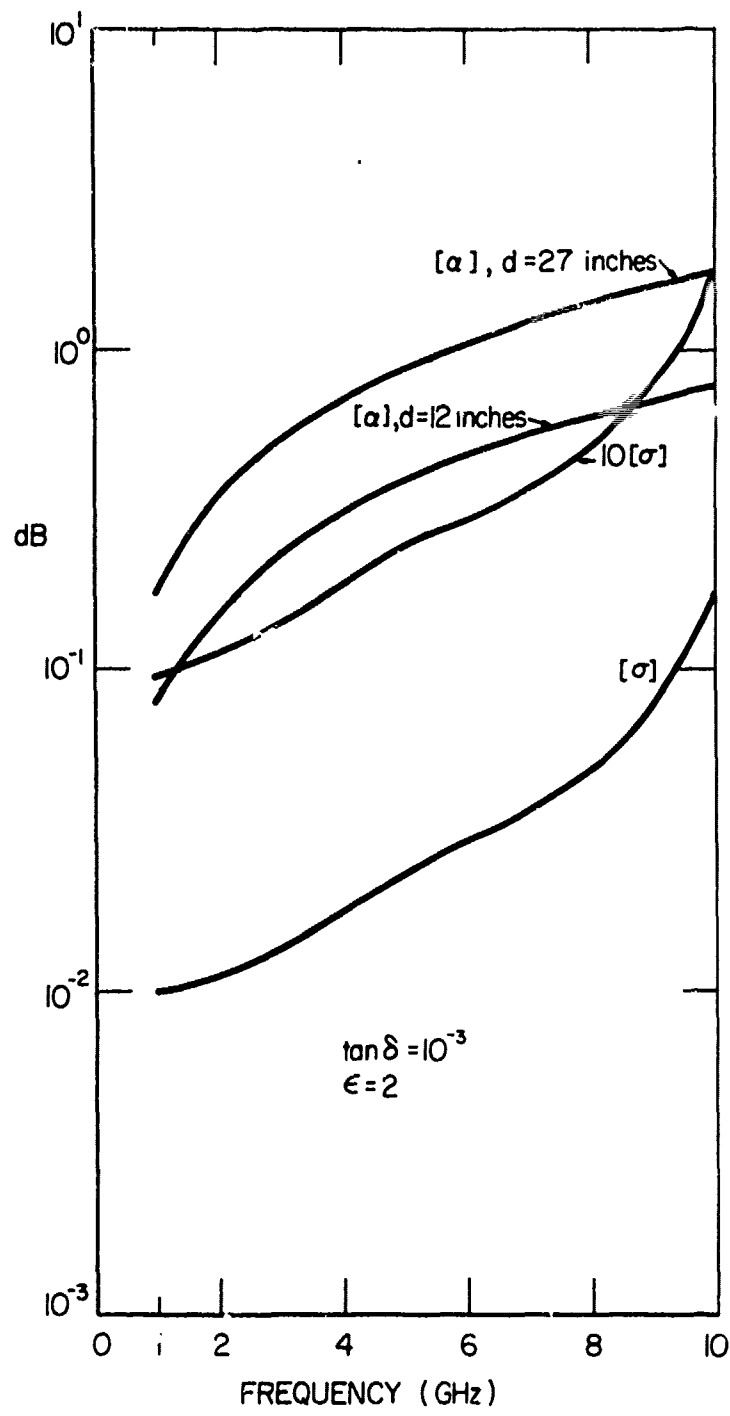


FIG. 10 Graph for determination of minimum sample length.



range and therefore is the minimum length sought.

Thus far the calculations have not accounted for copper loss in the portion of the line occupied by the sample. Since this loss depends on the dielectric constant in the line, it does not cancel out. When the copper loss approaches the order of the dielectric loss, it must be accounted for. Perhaps the most practical method of achieving this is through a computer correction of the measured data.

A variation of the long sample method, based on measurements of the reflections making four or six traverses of the sample, should be considered if the required sample length for the two traverse reflections becomes unwieldy. Sources of difficulty for this multiple pass method will be in making measurements where the incident pulses may not be in the same time window as the transmitted pulse and accounting for copper losses.

Strip line sample holders do not seem to offer any advantages over the coaxial line unless the material is only available in thin sheet stock. Even then it might be preferable to stamp disks from the sheet and mount a row of disks in the coaxial line. The higher order modes introduced at the stripline to coaxial junction will complicate the measurement interpretation.

In conclusion, the long sample method appears to be the best way at present to measure low loss materials. A long sample holder backed by a short circuit could be made to accommodate the sample. The measurement system should be versatile enough so that different sample lengths can be used. That is, longer samples will be required for materials with  $\tan \delta = 10^{-3}$  than for  $\tan \delta = 10^{-1}$ . The equations given in this section can be used to determine the lengths required. This versatility can be included by having variable position reference waveforms and variable time windows. It is suggested that another network configuration, compatible with the existing instrument rack, be built to perform the low loss measurements.

REFERENCES

- (1) A. M. Nicolson, P. G. Mitchell, R. M. Mara, A. M. Auckenthaler, "Time Domain Measurement of Microwave Absorbers", Technical Report AFAL-TR-71-353, Nov. 1971.
- (2) A. M. Nicolson, "Time Domain Measurement of Microwave Absorbers", Technical Report AFAL-TR-71-33, Feb. 1971.
- (3) S. Ramo and J. R. Whinnery, "Fields and Waves in Modern Radio", J. Wiley & Sons, Inc., New York, 1953, p. 310.
- (4) H. M. Cronson, P. G. Mitchell, J. L. Allen, "Time Domain Metrology Study", SRRC-CR-72-9, Aug. 1972.

## APPENDIX A

### REVISED MAIN PROGRAM WITH DISPLACED SHORT CORRECTION

The new main program is listed below. The data card with the displaced short distance of 400 mils should be inserted immediately before the sample thickness cards.

11:52:56

8FOR 9  
UNIVAC 418-117 RTOS/4 FORTRAN COMPILATION -- NOV 28 1972 11:52:57

```
1 C PROGRAM REVISED SEPT. 1972 TO INCLUDE DISPLACED SHORT CORRECTION
2 C DRIVER MUEP
3 C COMPUTE MU AND EPSILON ACCORDING TO AMN NOTES 4 FEB 71
4 C MODIFY S11 AND S21 ACCORDING TO MC NOTES 26 JULY 72
5 DIMENSION RA(1024),RB(1024),RC(1024)
6 *TA(2,1024),TB(2,1024),TC(2,1024),TD(2,1024)
7 *X(200),Y(200) *TE(2,1024),DE(1024)
8 *NA(300)
9 READ(5,10)FNOT,DELF
10 000020 READ(5,20)NMAX
11 000032 READ 10,DISP
12 000044 20 FORMAT(8F10.5)
13 000053 20 FORMAT(116Y3)
14 000061 WRITE(6,40)
15 000067 WRITE(6,10)FNOT,DELF
16 000105 WRITE(6,20)NMAX
17 000117 WRITE(6,11) DISP
18 000131 11 FORMAT(' DISP=',F10.5)
19 000143 40 FORMAT(' INPUT DATA'
20 000153 * FNOT,DELF')
21 000157 * NMAX*)
22 000163 NFOR=1024
23 000166 FC=45./ATAN(1.)
24 000202 NY=ATNT(FNOT/DELF+0.5)+1
25 000224 IF(N1.GT.1) GO TO 3
26 000233 N1=2
27 000236 FNO(=DELF
28 000242 3 CONTINUE
29 000242 NFS=NFOR/2+3
30 000251 NMAX=NIND(NMAX,NFS)
31 000260 N2=N1+NMAX-1
32 000263 50 FORMAT(' IFREQ(MHZ)*IX,*MU(REAL)*2X,*MU(IMAG)*
33 000303 *2X,*EPS(REAL) EPS(IMAG)*
34 000313 * MOD(REF) ARG(REF MOD(TRA) ARG(TRA)*
35 000331 * Z(REAL) Z(IMAG) GAM(REAL) GAM(IMAG)')
36 C CONVERT INPUT TO FYR ARRAYS AND TAKE XFORM
37 C RIB AND RBG
38 000351 CALL PECCV(IRA,NA,IER,4)
39 000357 IF(IER.NE.0) GO TO 401
40 000366 CALL PECCV(DE,NA,IER,4)
41 000374 IF(IER.NE.0) GO TO 401
42 000403 CALL PECCV(RB,NA,IER,4)
43 000411 IF(IER.NE.0) GO TO 401
44 000420 CALL PREP(TA,RA,RB,NFOR)
45 C RII
46 000426 CALL FTR(TA,NFOR,-1)
47 C TIB AND TBC
48 000433 CALL PREP(TE,DE,RB,NFOR)
49 000441 CALL FTR(TE,NFOR,-1)
50 000446 CALL PECCV(IRA,NA,IER,4)
```

```

51 000454      IF(IER.NE.0) GO TO 401
52 000463      CALL PECCV(RC,NA,IER,4)
53 000471      IF(IER.NE.0) GO TO 401
54 000500      CALL PREP(TB,RA,RC,NFOR)
55
56 000506      C TII
57 000513      101 CALL FTR(TB,NFOR,-1)
58 000513      101 CONTINUE
59 000531      1000 READ(5,1000) THIK,NSK
60 000531      1000 FORMAT( F10.5,I5)
61 000540      30 WRITE(6,30) THIK,DISP,NSK
62 000562      30 FORMAT(' THIK=',F10.5,' DISP=',F10.5,' NSK=',I5)
63 000604      IF(NSK.GT.0) CALL PECCV(RA,NA,IER,NSK)
64
65 000620      C ROB
66 000626      CALL PECCV(RA,NA,IER,4)
67 000635      IF(IER.NE.0) GO TO 401
68 000643      CALL PREP(TC,RA,RC,NFOR)
69
70 000650      C R00
71 000656      CALL FTR(TC,NFOR,-1)
72 000665      C T08
73 000673      CALL PECCV(RA,NA,IER,4)
74 000700      IF(IER.NE.0) GO TO 401
75 000707      CALL PREP(TD,RA,RC,NFOR)
76 000722      C T00
77 000730      CALL FTR(TD,NFOR,-1)
78 000736      FACB=5.3198E-7*THIK
79 000745      F=FN0T*(N1-2)*DEL
80 000745      FACB=1.8798E6/THIK
81 000752      WRITE(6,50)
82 000752      DAC=5.3198E-7*DISP
83 001006      DO 11 N=N1,N2
84 001021      *DIAGNOSTIC* THIS STATEMENT NUMBER IS DOUBLY DEFINED
85 001027      I=N
86 001035      CALL CPLEX(TA(1,I),TA(2,I),TE(1,I),TE(2,I),VR,VI,2)
87 001043      ALPH=2*DAC*F
88 001051      EXR=COS(ALPH)
89 001061      EXI=SIN(ALPH)
90 001072      UPR=EXR-VR
91 001072      UPI=EXI-VI
92 001127      DNR=VR-?
93 001135      CALL CPLEX(UPR,UPI,DNR,VI,PHOR ,RHOI ,2)
94
95 001142      C REF
96 001161      CALL CPLEX(TC (1,I),TC(2,I),TA(1,I),TA(2,I),REFR,REFI,2)
97 001201      C CHANGE SIGN REF
98 001226      REFR=-REFR
99 001237      REFI=-REFI
100 001273      C CORRECT WITH RHO
101 001304      CALL CPLEX(I,REFR,REFI,RHOR ,RHOI ,AR,AI,1)
102 001304      CALL CPLEX(REFR,REFI,AR,AI,REFR,REFI,2)
103 001304      RMOD=SQRT(REFR*REFR+REFI*REFI)
104 001304      RPH=ATAN2(REFI,REFR)*FC
105
106 001237      C TRA
107 001273      CALL CPLEX(TD(1,I),TD(2,I),TB(1,I),TB(2,I),BR,BI,2)
108 001304      CALL CPLEX(BR,BI,DR,DI,AR,AI,3)
109 001304      PHI=FACB*F

```

```

104 001313 CALL CPLEX(AR*AI,COS(PHI),-SIN(PHI),TRAR,TRAI,1)
105 001337 CALL CPLEX(REFR,REFI,RHOR ,RHOI ,AR*AI,1)
106 001350 AR=1.-AR
107 001357 AI=-AI
108 001364 CALL CPLEX(TRAR,TRAI,AR*AI,TRAR,TRAI,1)
109 001375 THOD=SQRT(TRAR*TRAR+TRAI*TRAI)
110 001422 TPH=ATAN2(TRAI,TRAR)*FC
111
112 001433 C V1,V2
113 001441 VIR=TRAR*REFR
114 001447 VII=TRAI*REFI
115 001455 AR=TRAR-REFR
116 AI=TRAI-REFI
117
117 001463 C X
118 001474 CALL CPLEX(VIR,VII,AR*AI,DR,DI,1)
119 001503 AR=1.-DR
120 001510 AI=-DI
121 CALL CPLEX(AR*AI,2.*REFR,2.*REFI,XR,XI,2)
122
122 001535 C GAMMA
123 001546 CALL CPLEX(XR,XI,XR*XI,BR,BI,1)
124 001555 BR=BR-1.
125 001566 CALL CPLEX(BR,BI,DR,DI,AR*AI,3)
126 001575 GR=XR*AR
127 001603 GI=XI*AI
128 001635 IF(SQRT(GR*GR+GI*GI).LE.1.) GO TO 9
129 001644 GR=XR-AR
130 001652 GI=XI-AI
131 9 CONTINUE
132
132 001663 C Z
133 CALL CPLEX(VIR,VII,GR*GI,AR*AI,1)
134 CALL CPLEX(VIR-GR,VII-GI,1.-AR,-AI,ZR,ZI,2)
135
135 001724 C C1
136 001757 CALL CPLEX(1.+GR*GI,1.-GR*-GI,C1R,C1I,2)
137 001770 CALL CPLEX(ZR,ZI,DUM,DUM,AR*AI,4)
138 002001 C2R=AR*FACB/F
139 002011 C2I=AI*FACB/F
140 002027 CALL CPLEX(C1R,C1I,-C2I,C2R,XMR,XMI,1)
141 002046 CALL CPLEX(-C2I,C2R,C1R,C1I,EPR,EPI,2)
142 002052 WRITE(6,60)F,XMR,XMI,EPR,EPI
143 002052 * ,RMOD,RPH,THOD,TPH
144 002140 * ,ZR,ZI,GR,GI
145 002151 60 FORMAT(F10.0,12F10.4)
146 002164 X(N)=F
147 002177 Y(N)=EPR
148 *DIAGNOSTIC* THIS STATEMENT NUMBER IS DOUBLY DEFINED
149 002206 11 CONTINUE
150 002214 NVAL=N2-N1+1
151 002221 CALL PLOT(1,X(NI),Y(NI),NVAL,J)
152 002246 J=J+1
153 002260 READ(5,10) MORE
154 002270 IF(MORE.GT.0) GO TO 101
155 402 CONTINUE
156 002273 STOP
157 401 WRITE(6,400)
158
157 002301 400 FORMAT(* FATAL ERROR*)
158 002312 GO TO 402
159 002314 END

```

116

## APPENDIX B

### REVISED CPLEX SUBROUTINE

In order to remove the incorrect angle computation as described in Section 4, the end of the CPLEX Subroutine in the original program should be modified as given below.

End of Original CPLEX Subroutine

```
5  AR = ALOG(R)
   AI = TH
   GO to 2
   END
```

Replace above statements with

```
5  AR = ALOG(R)
   AI = TH
   IF (AI. GT. 0.0) GO TO 6
   GO to 2
6  AI = AI - 6.28318
   GO to 2
   END
```